AN ABSTRACT OF THE THESIS OF

Marshall B. Field   for the M.A. in Physics
_____   _____   _____
     (Name)   (Degree)   (Major)

Date thesis is presented _November 3, 1966_

Title A THERMOELECTRIC STUDY OF DOPED LIQUID THALLIUM-

TELLURIUM ALLOYS

Abstract approved ████████████████████
                        (Major professor)

Electrical resistivity and thermoelectric power measurements
have been made over the temperature range of 450° to 600°C on
n-type liquid thallium-tellurium solutions. Liquids with compositions
from 67.5 to 72.0 atomic percent thallium were studied. In addition,
alloys of some of the three component thallium-tellurium solutions
containing small amounts of silver, cadmium, indium, tin (n-type
doping impurities), or antimony (p-type doping impurity) were studied.
The results suggest that each added atom of these doping elements
contributes some fractional number of a donor (or acceptor) level.
In addition, some measurements were made in a fused silica cell at
temperatures up to 875°C.

The data are analyzed using a conventional solid state transport
theory. This analysis yields the relative concentration and electron
mobility as a function of composition. P-n transitions in the Seebeck
coefficient at high temperature for some near intrinsic

thallium-tellurium solutions show that the electron mobility is larger

than the hole mobility at high temperatures. Other results included

estimates of the activation energies for holes in n-type solutions at

two compositions, and the electrical determination of a liquidus in

part of the phase diagram of the thallium-tellurium binary system.

A THERMOELECTRIC STUDY OF DOPED LIQUID
THALLIUM-TELLURIUM ALLOYS

by

MARSHALL B. FIELD

A THESIS

submitted to

OREGON STATE UNIVERSITY

in partial fulfillment of
the requirements for the
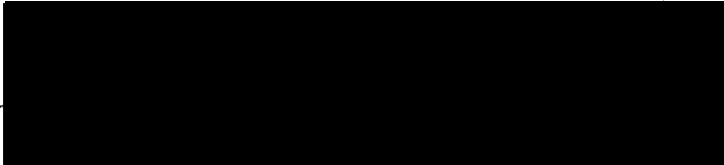degree of

MASTER OF ARTS

June 1967

APPROVED:

_____
Associate Professor of Physics

In Charge of Major

_____
Chairman of Department of Physics

_____
Dean of Graduate School

Date thesis is presented _____

Typed by Marion F. Palmateer

TABLE OF CONTENTS

LIST OF FIGURES

LIST OF TABLES

A THERMOELECTRIC STUDY OF DOPED LIQUID THALLIUM-TELLURIUM ALLOYS

INTRODUCTION

Although the existence of liquid semiconductors has been established for some time, there have been relatively few experiments performed with the aim of relating their properties to theory. This is due partly to the practical difficulties involved in performing experiments on liquids at high temperatures and the fact that the electronic theory of liquids is not so well-founded as the solid state theory. Ioffe and Regel (1960) have written a useful review which covers most of the work in this field. Much of the early work reported was aimed at merely establishing the existence of liquid semiconductors. From a relatively large body of data on solutions containing selenium or tellurium the physical structure of these liquids seems to be well understood. The electronic properties of liquid semiconductors are not well defined. Ioffe and Regel (1960) have offered as a criterion that an electrical conductivity, σ, of 10 to 10^4 mho/cm. necessarily implies semiconductor transport. This they contrast with ionic transport, $\sigma < 10$ mho/cm, and metallic transport, $\sigma > 10^4$ mho/cm. The mechanism of electronic transport in liquid semiconductors is still open to many questions.

Very little theoretical work has been published that deals with the transport properties of liquids. The bulk of the papers in the

literature deal with one-dimensional models. On the other hand, the usual solid state transport theory is not clearly applicable to liquids. The conventional transport theory assumes that the mean free path of the carriers is longer than the de Broglie wave length. This is not true for most liquids. Any predictions of solid state theory which depend on long range order would not obviously apply to liquids. In spite of these fundamental defects in conventional theory vis a vis liquids, the theory does describe the behavior of liquid semiconductors in some respects. The existence of energy bands in liquid semiconductors is well established, for example (Ioffe and Regel, 1960, reference 79). In this paper we will analyze some of the data for thermoelectric measurements as a function of temperature and concentration on doped thallium-tellurium solutions, making use of standard solid state transport theory. It will be demonstrated that much of the data can be successfully fitted into the framework of conventional theory.

Semiconducting solutions of liquid thallium-tellurium were first studied by Stoneburner (1965), who measured the Seebeck coefficient and the electrical conductivity as a function of temperature for two compositions corresponding to the solid compounds Tl_2Te_3 and $TlTe$. Cutler and Mallon (1965) reported data for the same parameters and the thermal conductivity over a wide range of temperatures and compositions. During their investigations they observed a transition in the electrical conductivity from conduction by holes to conduction by

electrons (a p-n transition) at a composition of about 66.5 atomic percent thallium. In a recent paper by the same authors (Cutler and Mallon, 1966) their data was extensively analyzed using the equations of conventional transport theory.

Cutler and Leavy (1963) conducted some doping studies with indium, iodine, bismuth, and selenium in solutions of thallium-tellurium near the 31.0 atomic percent thallium eutectic. This is in the p-type conduction region. Their data showed that these elements had little or no effect on the resistivity or Seebeck coefficient. Cutler (1963) pointed out that this immunity to doping was probably due to a strong electronic buffering action at this composition. Later work (Cutler and Mallon, 1966) showed that tellurium in excess of the intrinsic composition (66.7 atomic percent thallium) produced deep-lying acceptor states which are only slightly ionized. In the near intrinsic and n-type compositions we might expect that the impurity states would be largely ionized. If this is so, these compositions should be sensitive to the addition of impurity atoms. As shown below, solutions of thallium-tellurium with more than 66.0 atomic percent thallium are indeed sensitive to doping.

This paper presents some of the results obtained through measurements of the electrical conductivity and thermoelectric power as a function of temperature and composition on liquid thallium-tellurium solutions. For the most part, data which falls in the area

of compositions greater than 67. 5 atomic percent thallium will be

shown.   Two types of experiment were performed and analyzed:

1) the behavior of two component thallium-tellurium solutions in the

n-type and intrinsic region, 67. 5 to 72. 0 atomic percent thallium was

carefully studied, and 2) the effect of small amounts of an added third

element on the thermoelectric parameters of these thallium-tellurium

solutions was examined for a number of elements.   Some of this data

was analyzed in terms of conventional transport theory.   The various

doping elements were compared with tellurium and thallium with

regard to effectiveness and direction of doping.

EXPERIMENTAL METHOD

The apparatus and techniques used in this experiment were developed largely by Cutler and Mallon (1965). Some refinement of the experimental method was carried out in the present work. The general method of measurement is reviewed below; a detailed account of those aspects of the experimental technique which go beyond the report of Cutler and Mallon (1965) is presented in Appendix 1.

The measuring cell was constructed of pyrex glass, usually, although some were built of fused silica. The cell has four electrodes sealed in a line into the side of a small diameter closed tube at the bottom of the cell. This electrode region is connected to a larger tube, the reservoir, which in turn is sealed to a long pyrex tube terminating in a male ground glass joint. A cap fits on the ground glass joint and has provisions for evacuating and back-filling the cell with gas. Figure 14 (page 52) includes a sketch of the Seebeck cell and cell cap. The two outer electrodes are current leads. Pt_{100} - $Pt_{90}Rh_{10}$ thermocouples are attached to the two inner electrodes. After assembly the cell is inserted into a tube furnace which has a temperature gradient in the electrode region. The thermocouples measure ΔT, the temperature difference between the two inner electrodes, and one leg of each thermocouple is used as a voltage probe to measure the thermoelectric potential and the voltage

drop across the sample.

In the beginning of this project the pyrex cells broke frequently while cooling to room temperature after a series of measurements. There was indirect evidence which indicated that the cause of breakage was partly due to metal oxides adhering to both the frozen melt and the glass walls. As the cell cooled the differences in the thermal expansion coefficients were such that the stresses developed would crack the glass. Several steps were taken to ensure that the cell and the melt remained oxygen-free. Among these were 1) cleaning the glassware very carefully, 2) maintaining a dry argon atmosphere in the cell, and 3) removing most of the oxide from the thallium before depositing it into the cell. Very pure thallium is available commercially, but since thallium oxidizes readily it must be further cleaned by causing the molten metal to flow through a series of glass funnels. The oxide adheres to the glass, and the pure metal is subsequently deposited into the measuring cell. A carefully weighed amount of tellurium was placed in the cell at room temperature, before the thallium was added. Once the thallium had been deposited the cell was not allowed to cool during the course of measurements. This further minimized cell breakage. A series of measurements typically encompassed some eight or nine distinct compositions and lasted four or five days. This procedure necessitated the invention of special methods for accurately adding small amounts of material

to the hot melt, and for controlling the amount of thallium deposited
into the cell. These methods are detailed in Appendix 1. At the con-
clusion of an experiment, the melt was largely removed before the
cell was allowed to cool.

After the thallium was deposited into the cell, the solution of
thallium and tellurium was thoroughly mixed by tilting the furnace
and alternately running the liquid between the electrode region and
the reservoir. Solutions were mixed until reproducible results of
resistivity at a given temperature were obtained. This typically re-
quired some number above one hundred tilts. Measurements were
taken at both increasing and decreasing temperatures. It was found
that the rate of cooling or heating could affect the accuracy of the
results. If the rate of temperature increase or decrease was greater
than $3°C$ per minute, the data showed a great deal of scatter. The
temperature difference between the thermocouples was about $25°C$
and varied slightly during the course of measurements ranging from
$470°C$ to $600°C$. The thermocouples were connected to an electric
switch whose output was in turn fed to a Sargent chart recorder.
The switch alternated between the two thermocouples every 30
seconds. The temperature difference, ΔT, could then be read direct-
ly from the chart. The average temperature was interpolated as the
temperature halfway between the two readings on the chart.

The thermoelectric voltage, $S\Delta T$, was measured across the

inner two tungsten electrodes with no current flowing. The voltage, measured with a Biddle potentiometer, was thus a separate measurement from that of ΔT. The Biddle potentiometer has a quoted accuracy of 0.05 percent of the reading plus 1.6 microvolts; the chart recorder is accurate to 0.1 percent. This leads to an estimated uncertainty of $\pm$ 3 percent in the thermoelectric power and the resistivity. S, the Seebeck coefficient, measured with respect to the metal in the voltage probe, is later converted to an absolute scale.

With a current flowing between the two outer electrodes the voltage drop across the inner two electrodes was measured with the potentiometer and averaged for currents running in both directions. This allowed the separation of the thermoelectric voltage from the voltage caused by the electrical resistivity. The geometrical constant of the cell for resistivity measurements was calibrated before each run by measuring the resistance of pure mercury at room temperature. Since the resistivity of mercury is well known, the cell constant could be calculated.

Most of the cells used in this experiment were constructed of pyrex glass. Pyrex has many desirable features for work of this kind such as chemical inertness, ease of working, and low coefficient of thermal expansion, but its use constrains the experimenter to temperatures below the softening point, 600°C. Since many of the compositions studied do not melt below 450°C, pyrex cells severely restrict

the temperature range of the data. Fused silica (quartz glass) cells would allow measurements up to 1000°C. It is possible to construct quartz cells having sealed tungsten electrodes similar to those in the pyrex cells. Quartz cells of this type proved unsatisfactory for repeated measurements at high temperatures, as discussed in Appendix 1, because of poor reproducibility in the data obtained from them. At high temperatures, it appears that thallium-tellurium solutions corrode tungsten electrodes. The electrical properties of the corrosion product apparently cause the erratic and nonreproducible data which were obtained. The bulk of the data reported here was obtained with pyrex cells in the temperature range 450 - 600°C.

EXPERIMENTAL RESULTS

The basic data which were obtained were ρ, the electrical resistivity, and S, the Seebeck coefficient, as a function of temperature for a given composition. After adding a small amount of a third element, or more tellurium, the measurements were repeated. Graphs of ρ and S versus temperature can then be drawn for the different compositions. The thallium-tellurium solutions are labelled as X, followed by a number giving the atomic percent of thallium in the solution.

$$X = 100 \; N_{Tl}/(N_{Tl} + N_{Te}).$$

N_{Tl} is the number of gram atoms of thallium in the solution.

$$N_{Tl} = m_{Tl}/W_{Tl}.$$

$$m_{Tl} = \text{weight of thallium in grams.}$$

$$W_{Tl} = \text{atomic weight of thallium.}$$

Compositions which have been doped with a third element are characterized by the original thallium-tellurium composition plus A_i. A_i is the atomic percent of the third element, and i is the symbol for the third element.

$$A_i = 100 \; N_i/(N_{Tl} + N_{Te} + N_i)$$

A typical experimental melt, then, would be listed as X66. 0 - A_{Cd} = 1. 30. This reads "sixty-six atomic percent thallium plus

one and three-tenths atomic per cent cadmium". Addition of a third

constituent changes X_{Tl}, of course, but this change is relatively

small, and is conveniently neglected.

In the earlier experiments of Cutler and Mallon (1965), the

control over the composition of the melt was limited. They quoted an

uncertainty of ± 0.5 atomic percent in their compositions. In the

work reported here, the uncertainty in the composition is estimated

as ± 0.1 atomic percent. The improved method of thallium deposi-

tion and doping, as detailed in Appendix 1, is the source of the in-

creased accuracy.

An interesting feature of liquid thallium-tellurium compounds

is the transition from electrical conduction by electrons to conduction

by positively charged carriers (holes) as the composition is changed.

The sign of the current carriers is determined by the sign of the

Seebeck coefficient, as will be shown below. If the concentration of

thallium is less than X66.8 the conduction is by holes (p-type); at

compositions greater than X66.8 the conduction is by electrons

(n-type).

The resistivity and Seebeck coefficient of liquid thallium-tel-

lurium solutions were measured for compositions ranging from X67.5

to X72.0. Figures 1 and 2 show the conductivity, σ (T) defined as

$1/\rho$, and the Seebeck coefficient, S(T), for a number of the n-type

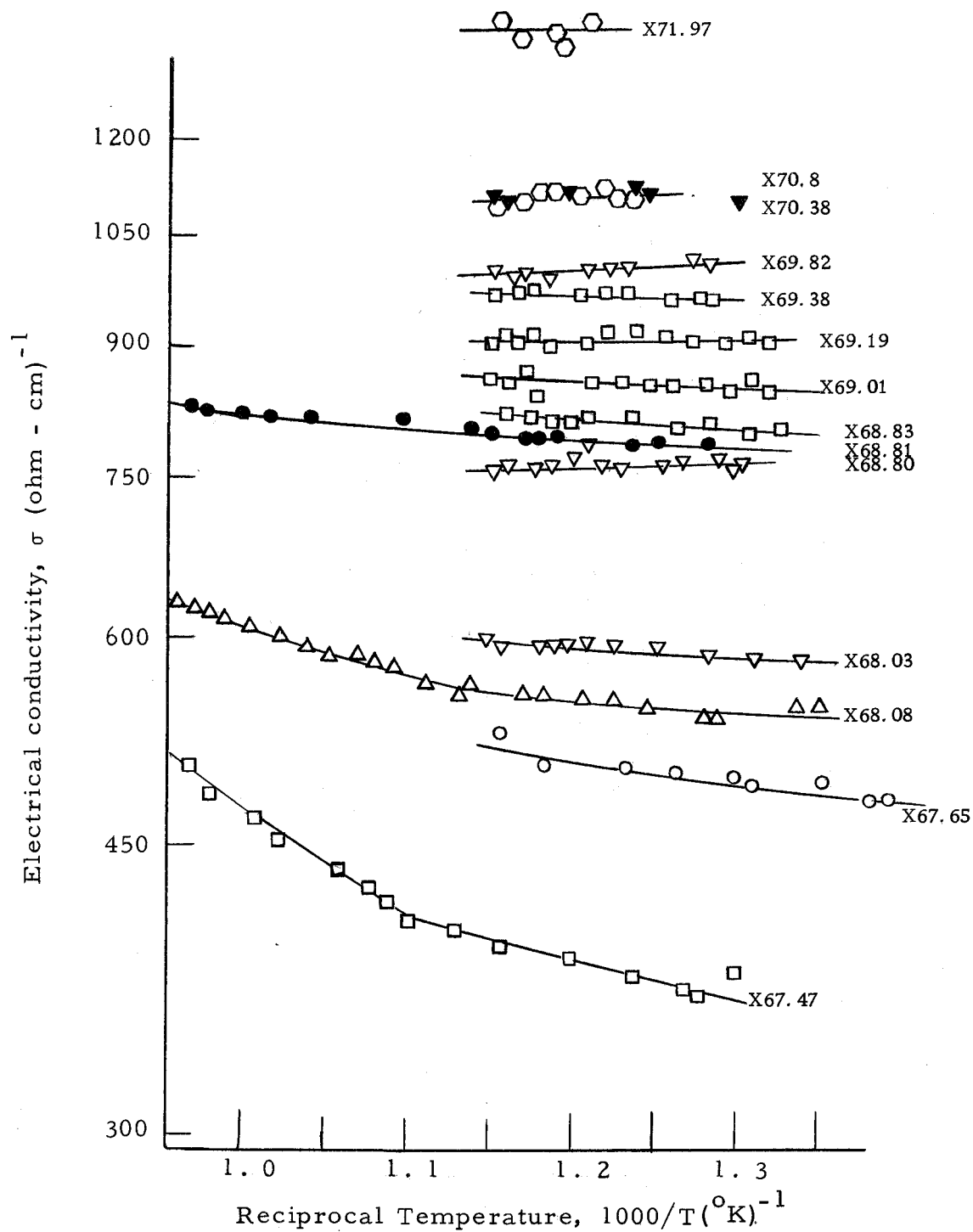thallium-tellurium solutions. The composition of the melt is

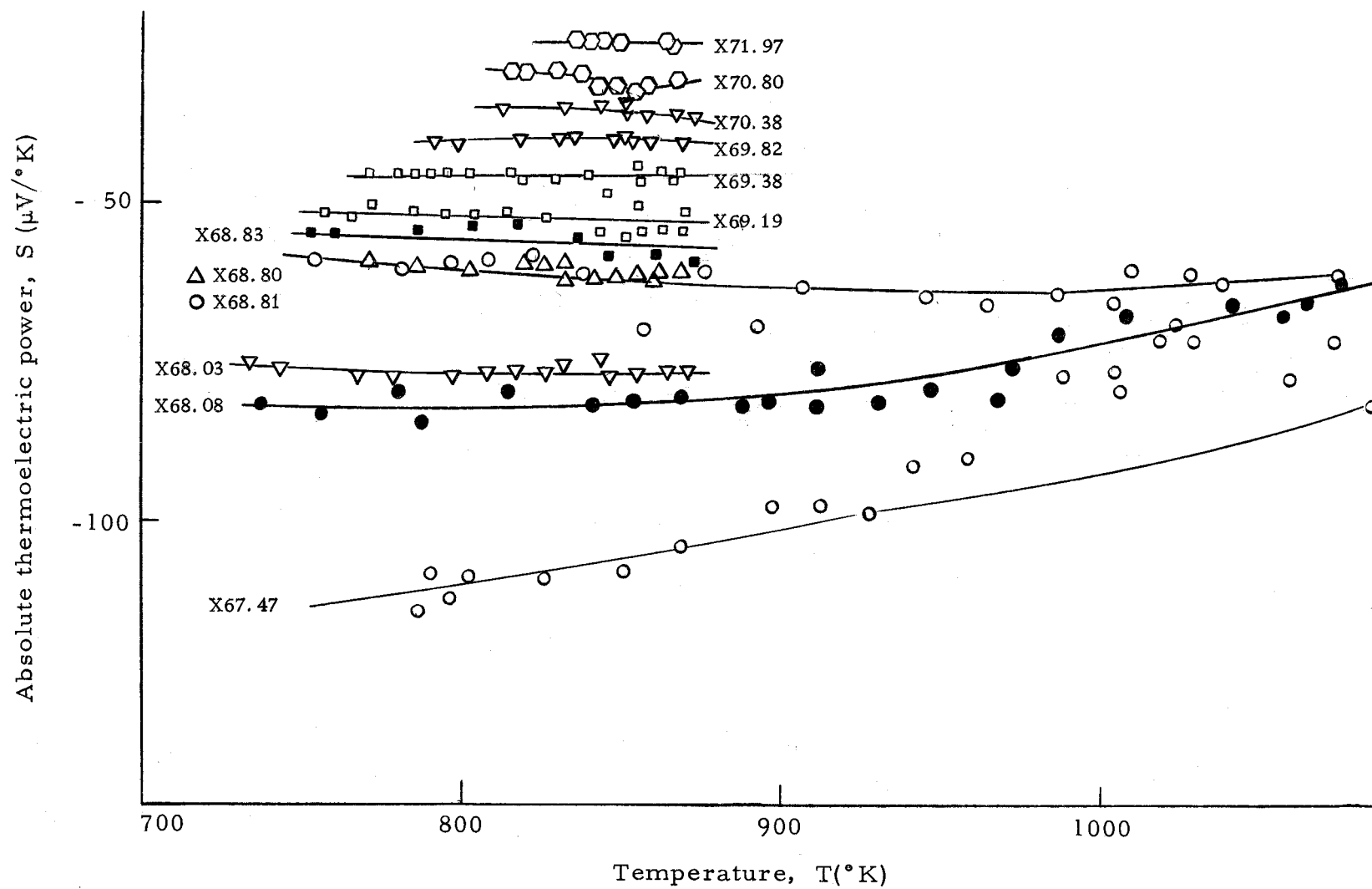Figure 1. Electrical conductivity of some n-type thallium-tellurium compositions.

Figure 2. Seebeck coefficient of some n-type thallium-tellurium compositions.

determined to within ± 0.1 atomic percent, but two sources of random error can cause scatter in the composition: (1) Unless the melt is mixed thoroughly, the liquid will not be homogeneous, (2) When mixing, any splatter which adheres to the top of the cell, or any vapor which subsequently condenses in the cold region, will remove material from the melt and change the composition. In general, σ has a minimum at the lowest temperature and increases with increasing temperature. The magnitude of S decreases with increasing temperature. This is consistent with the behavior of other liquid semiconductors reviewed by Ioffe and Regel (1960).

A method of showing explicitly the effect of composition on the conductivity and Seebeck coefficient is to plot isothermal curves of S and σ versus X. Figures 3 and 4 show such plots at 800 degrees Kelvin for the range X60 to X72. The Seebeck coefficient changes sign at about X66.7. The minimum in the conductivity occurs close to the value of X where S is zero. Cutler and Mallon (1966) pointed out that this behavior is typical of a transition between n-type and p-type conduction, and that the intrinsic composition corresponds closely to the stoichiometry Tl_2Te. The value of the inversion composition reported here is more accurate than the value determined by Cutler and Mallon (1966). On the basis of several different measurements in this region, both in pyrex and in quartz cells, the inversion composition lies between X66.5 and X66.86. The temperature range
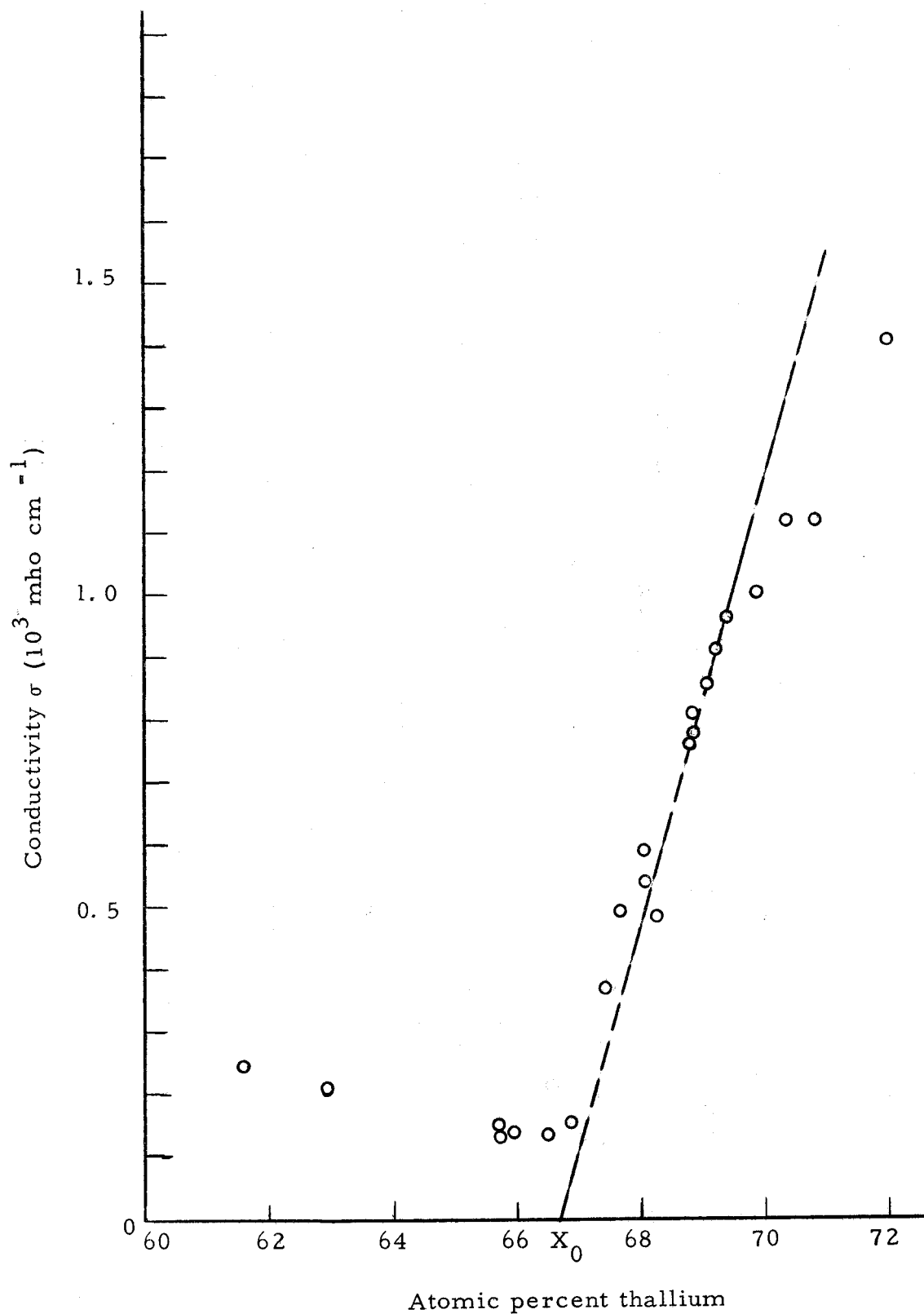
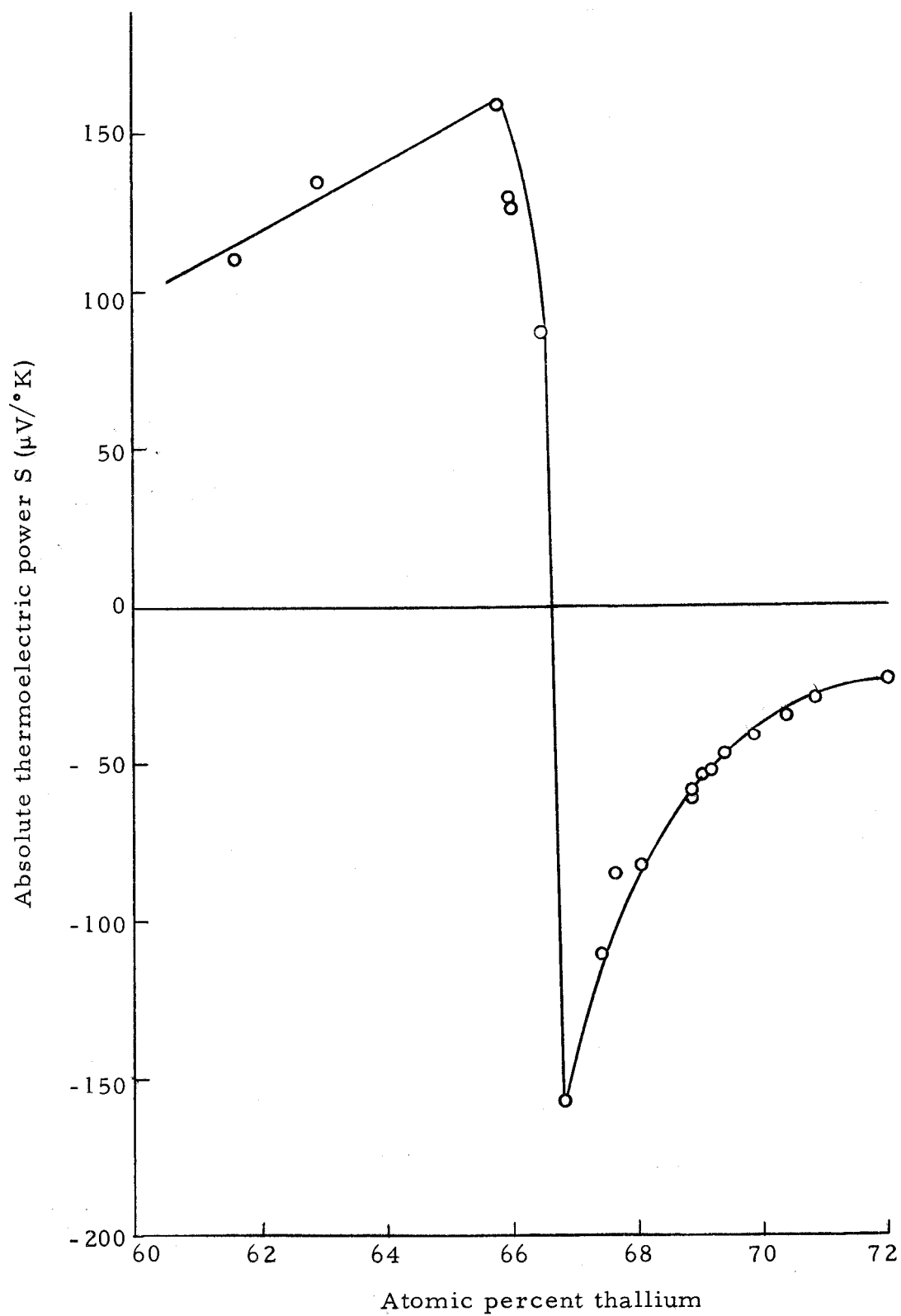Figure 3. Isothermal plot of σ versus thallium-tellurium composition at $T = 800°K$.

Figure 4. Isothermal plot of S for some thallium-tellurium compositions at T = 800° K.

of the data was 470°C to 850°C.

Table lists the doping experiments reported here in which a third element was added to n-type thallium-tellurium compositions. X is the original, undoped composition, which was then doped with the element listed on the right. In some cases, several doping experiments were performed with the same element but different X. The table refers to one particular experiment with this element which is typical of the others. Data obtained by doping p-type thallium-tellurium solutions are not reported; the directions of the doping effect were the same as those shown below.

Table 1. Doping experiments performed.

X	Doping element	Range of A_i, at. %	Doping type
68.32	Ag	0 - 3.58	n
68.03	Cd	0 - 2.16	n
66.86	In	0 - 3.62	n
67.65	Sn	0 - 2.06	n
68.83	Sb	0 - 2.52	p

Figures 5 and 6 show the results of a doping experiment with cadmium in a pyrex glass cell. These curves are representative of those obtained in the other doping experiments. Starting with $X = 68.03$, cadmium was added in amounts ranging from $A_{Cd} = 0.39$ to $A_{Cd} = 2.16$,
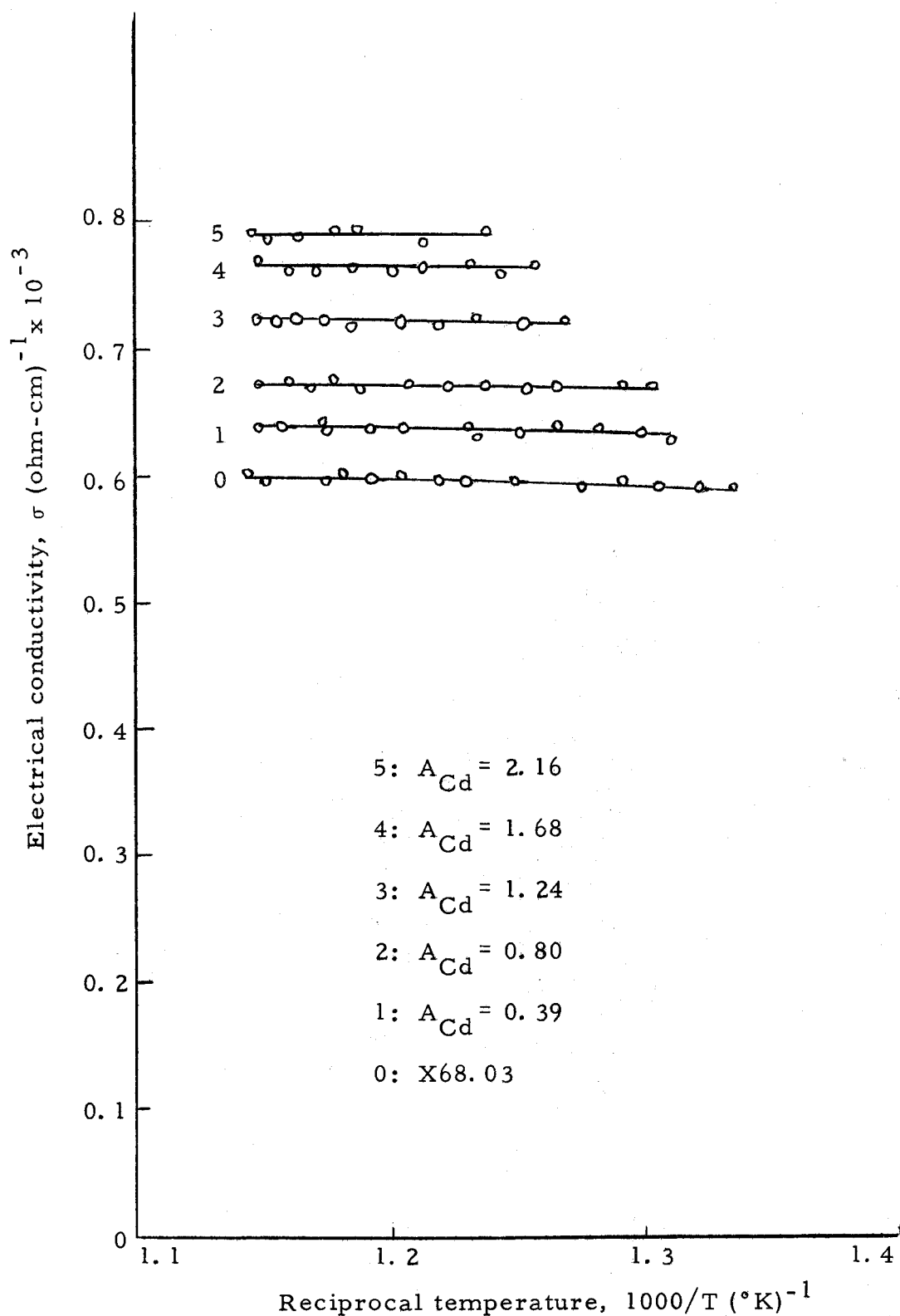
Figure 5. Electrical conductivity for a cadmium doping experiment.
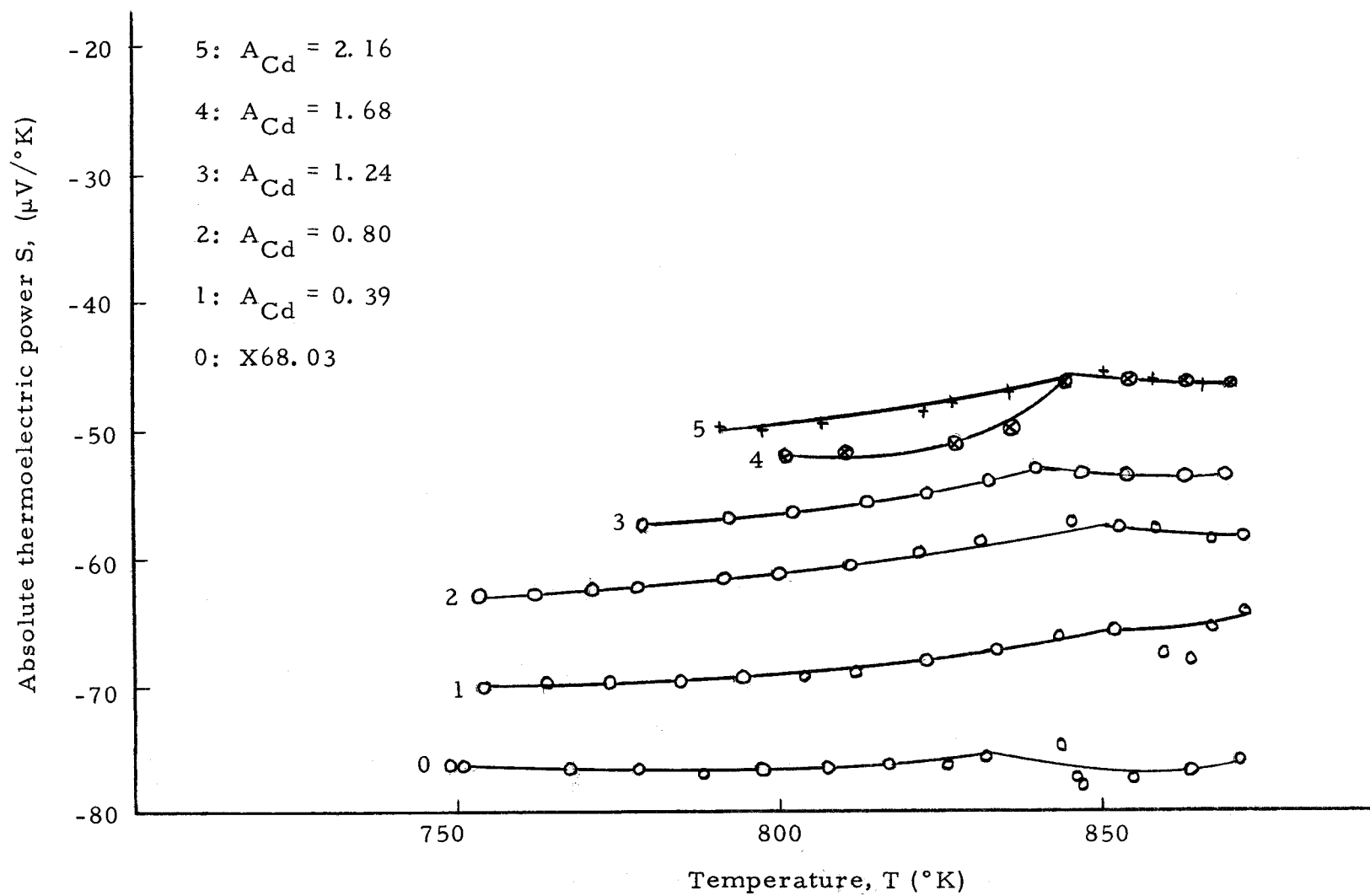
Figure 6. Seebeck coefficient for a cadmium doping experiment.

in five steps.   The original, undoped composition was n-type and

extrinsic, as shown by the temperature dependence of the conductivity

and the sign of S.   The addition of cadmium increased the conductivity,

but left the temperature dependence essentially unchanged.   The mag-

nitude of S decreased as cadmium is added, showing that the effect

of cadmium in solution was to increase the number of electrons. Each

cadmium atom gives up some number (possibly fractional) of elec-

trons.   Cadmium is thus an n-type doping impurity in Tl_2Te.   Indium,

tin, and silver have similar behavior, although the magnitude of the

change in conductivity was quantitatively different in each case.

Antimony and bismuth are p-type doping agents.   Small amounts of

these elements, added to extrinsic thallium-tellurium, initially

decrease the conductivity.   As the amount of doping agent (Sb, Bi, Te)

in solution increases, the temperature dependence of the conductivity

is modified as well.   The data on bismuth doping are incomplete as

yet and are not included here.   It is definitely a p-type impurity, but

quantitative results are lacking.

The experiments with thallium-tellurium alloys also yielded

information about the phase diagram.   As the temperature of the melt

was decreased during the course of an experiment, a temperature was

reached at which it was no longer possible to balance the potentiometer;

the electrical parameters of the system were changing too rapidly.

This phenomenon was interpreted to mean that a phase separation

was occurring. The electrical parameters were changing as another phase with a different composition precipitated out of solution. Determination of phase transition points by methods like this is often used by metallurgists. If the temperature at which the erratic behavior first occurs is recorded, along with the composition of the liquid, it is possible to draw the thallium-tellurium liquidus. Figure 7 is a plot of the liquidus determined by our measurements. The dashed curve is a portion of the liquidus published by Elliot (1965). The minimum of the curve, which indicates a eutectic, could lie between X67 and X68 on the basis of the data. Elliot (1965) places it at about X68. 5.
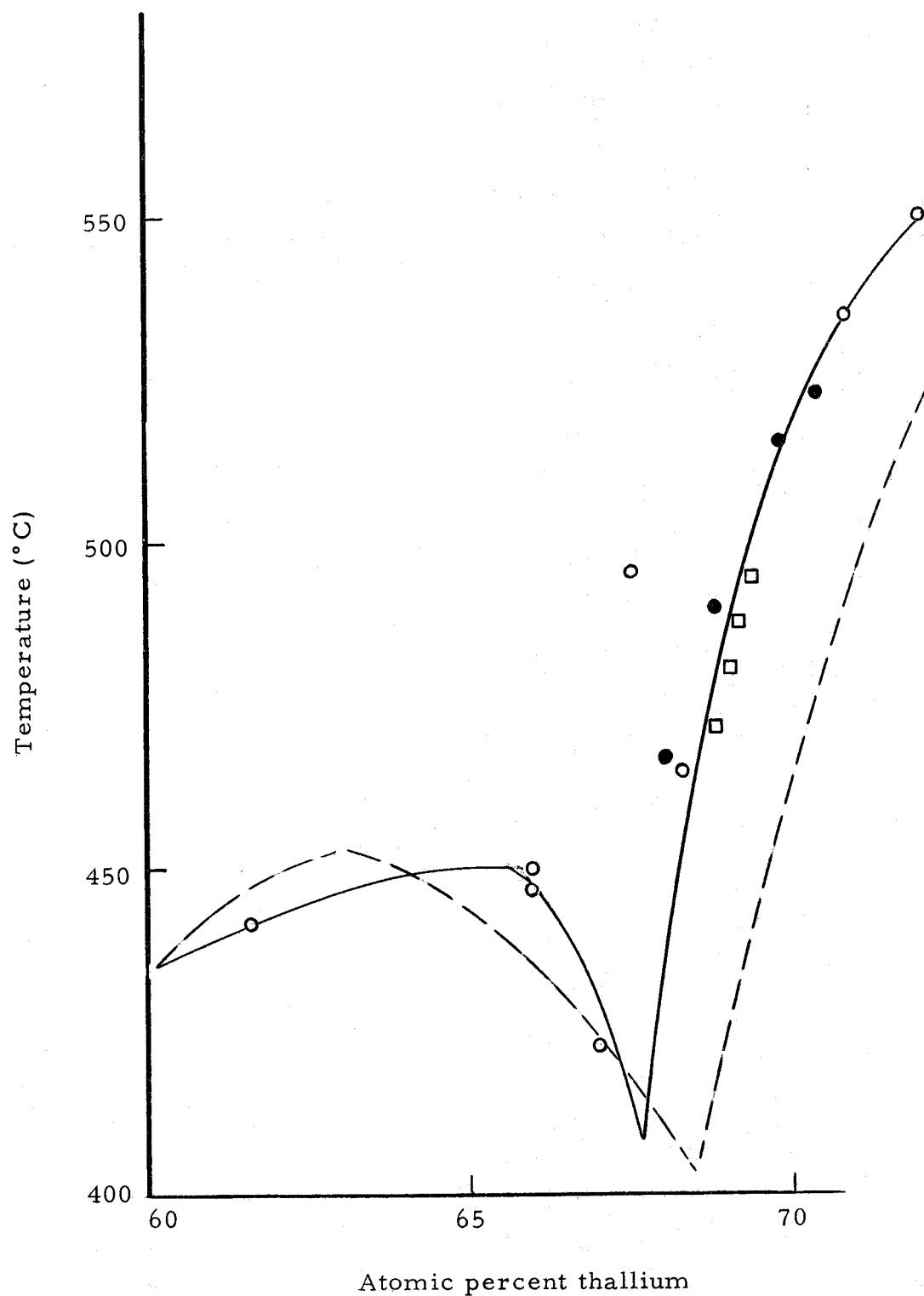
Figure 7. A portion of the liquidus of thallium-tellurium determined from electrical measurements.

THEORY AND ANALYSIS

In this section, some of the experimental results will be analyzed using conventional solid state theory. The conventional transport equations are solutions of the Boltzmann equation, assuming a relaxation time for scattering which is at most a function of energy. The equations are written in terms of an effective mass, so their form also includes the hypothesis that there is a conventional band, i. e., the electron energy is a quadratic function of its wave vector. These assumptions, and others, are built into the equations used below. Other assumptions which apply to specific portions of the analysis will be mentioned in the appropriate part of this paper. A good review by Fan (1955) derives most of the relations used here and discusses to some extent the conventional theory. For further details see Kittel (1960) or Seitz (1940).

Transport theory predicts the behavior of the electrical conductivity and Seebeck coefficient as a function of temperature, concentration of carriers, and as influenced by the scattering mechanism. In the present measurements, the temperature and concentration are varied. There is a limitation on the type of analysis which is possible due to the fact that this experiment does not furnish mobilities or concentrations directly. An indirect method is used to determine the change in the mobility and concentration with X, or A, which yields

only the relative values of these quantities.

The electrical conductivity when two carriers are present is

$$\sigma = ne\mu_n + pe\mu_p. \tag{1}$$

n = concentration of electrons.

p = concentration of holes.

μ = mobility.

e = magnitude of the electronic charge.

The electrons and holes obey the equilibrium relation

$$n\,p = N_c N_v \exp(-E_G/kT) \equiv n_i^2. \tag{2}$$

N_c is the effective density of states in the conduction band, N_v is the effective density of states in the valence band:

$$N_c = 2(2\pi m_n^* kT)^{3/2}/h^3, \tag{3}$$

$$N_v = 2(2\pi m_p^* kT)^{3/2}/h^3.$$

E_G is the energy difference between the bottom of the conduction band and the top of the valence band. Assuming that

$$n = N + p, \tag{4}$$

where N is the effective density of ionized centers, then

$$\sigma = Ne\mu_n + e(\mu_n + \mu_p)p,$$

$$= Ne\mu_n + e(\mu_n + \mu_p)\frac{N_c N_v}{(N+p)} \exp(-E_G/kT). \tag{6}$$

Let $\dfrac{\mu_p}{\mu_n} = b$, $\sigma_N = e\mu_n N$. Then we can write

$$\sigma = \sigma_N + \frac{e\mu_n(1 + b)}{N + p} \, N_c N_v \exp(- E_G/kT). \tag{7}$$

The first term, σ_N, may be expected to vary linearly with X. This is a hypothesis which will be examined in the present study.

The Seebeck coefficient, S, is the sum of the thermoelectric power of the holes and that of the electrons.

$$S = f(n) + f(p) \tag{8}$$

Equation (8) can be written so as to show explicitly the balance between holes and electrons.

$$S = S_n \frac{\sigma_n}{\sigma} + S_p \frac{\sigma_p}{\sigma}. \tag{9}$$

S_p is a positive quantity; S_n is negative. In the Maxwell-Boltzmann limit S_n and S_p have the form

$$S_n = -\frac{k}{e}(A_n + \ln \frac{N_c}{n}),$$

$$S_p = \frac{k}{e}(A_p + \ln \frac{N_v}{p}). \tag{10}$$

A_n and A_p are constants whose value is determined by the scattering mechanism. The Boltzmann constant is k. Equation (10) applies in the intrinsic conduction region, where the Fermi energy is near the center of the band gap. As the number of electrons contributing to transport increases it is necessary to apply Fermi-Dirac statistics. Then

$$S_n = -\frac{k}{e}\left[(r + 5/2) \frac{F_{r + 3/2}(\zeta)}{F_{r + 1/2}(\zeta)} - \zeta\right] \tag{11}$$

The functions $F_\alpha(\zeta)$ are Fermi-Dirac integrals, as tabulated by Blakemore (1962), and others. ζ is equal to the difference between the Fermi energy and the energy of the bottom of the conduction band, divided by kT. The parameter r depends on the scattering time and is defined later. The definition of $F_\alpha(\zeta)$ may be found in equation A(8), page 55, Appendix 2.

The analysis divides itself conveniently into two separate regions according to composition. Thallium-tellurium solutions near X66.0 are intrinsic or nearly intrinsic in their conduction properties. In this first region, they are non-degenerate semiconductors, and Maxwell-Boltzmann statistics should apply. The analysis of the experimental results in this area is complicated by the fact that there are nearly equal numbers of holes and electrons, which are changing rapidly with temperature. As a result, σ and S are strong functions of temperature. As the concentration of thallium is increased, the relative contribution of holes to transport decreases rapidly. The second region is at compositions above about X68.0, where the electronic behavior is extrinsic. Plots of conductivity versus temperature are nearly horizontal straight lfnes over the entire range. For these compositions the number of electrons should be nearly equal to the number of ionized donor states.

Extrinsic Region

In the analysis of the extrinsic conduction region of thallium-tellurium solutions, we make the following assumptions: (1) the donor states are fully ionized, (2) the concentration of donor states changes in proportion to X or A, and (3) the ionization state of the donor ion doesn't change during the course of an experiment. It is shown below that the data are consistent with these assumptions. In this region $p << N$, $n \sim N$, and

$$\sigma \cong e\mu_n N \equiv \sigma_N, \tag{12}$$

$$\Delta N = a \Delta X$$

and
$$N = N_0 + a X. \tag{13}$$

N_0 is the density of donors at some reference point. Thus,

$$\sigma = \sigma_{N_0} + e\mu_n a X. \tag{14}$$

If we add a third element to extrinsic thallium-tellurium solutions, equations (13) and (14) should hold upon replacing X by A_i, the atomic percent of the doping element, and N_0 becomes the value of N at the composition for A = 0.

The change in the electron concentration with composition is derived from the Seebeck coefficient S. As long as the scattering mechanism is unchanged, S does not depend on μ. The dependence on n can be expressed in the form

$$(S + \frac{3}{2} \ln T)\frac{e}{K} = \ln n + const. , \tag{15}$$

where the unknown constants have been lumped together. As a result, a knowledge of S as a function of X (or A) at a given T determines the value of n(X) to within an unknown constant. The behavior of S in this region is described more accurately by Fermi-Dirac integrals, as shown in detail in Appendix 2, rather than equation (15), which corresponds to the Maxwell-Boltzmann limit. In terms of Fermi-Dirac integrals the form of S_n is that of equation (11). ζ is related to n by

$$n/N_c = F_{1/2}(\zeta). \tag{16}$$

The parameter r is determined from the energy dependence of τ, the scattering time, by the relation $r = d \ln(\tau)/d \ln E$. E is the kinetic energy of the electrons (see Appendix 2). We can formally express the dependence of $S\frac{e}{K}$ on the concentration by writing

$$n/N_c = f_r(S\frac{e}{K}). \tag{17}$$

Now, in analogy to equation (15),

$$\ln f_r(S\frac{e}{K}) = \ln n - \ln(const.) - 3/2 \ln T. \tag{18}$$

Using equation (18), a graph of S versus ln T can be drawn for an arbitrary value of $n = n_R$, if a value of r is assumed. In plotting this curve, $r = -1/2$, corresponding to thermal scattering, was used. This is not a critical assumption, since an error in the value of r

leads, to a good approximation, to a horizontal shift in the curve. This is equivalent to a change in the unknown constants.

Values of $n(X)/n_R$ were calculated by comparing experimental results with the curve drawn using equation (18). Picking a ratio from the data, $n(68.03)/n_R$, and referring all others to it, allows us to plot $n(X)/n(68.03)$ versus X at a given temperature. Such a plot shows a reasonable straight line, as shown in Figure 8. This indicates that ΔN is proportional to ΔX, as assumed.

A more interesting curve is shown in Figure 9. This is a graph of $\sigma(X)/\sigma(68.03)$, obtained from the conductivity data at $T = 800°K$, versus $n(X)/n(68.03)$. This is a curve of $\left(\mu(X)/\mu(68.03)\right) \cdot \left(n(X)/n(68.03)\right)$ versus $n(X)/n(68.03)$ and hence the slope is $\mu(X)/\mu(68.03)$. The curve lies along a straight line at a slope of 45 degrees for lower X, and then falls below it. This indicates that $\mu(X) = \mu(68.03)$, to a good approximation, for compositions from X67.0 to X68.5. For compositions rich in thallium the curve bends down nearly horizontal, indicating the electron mobility is decreasing with further additions of thallium. Upon close inspection of Figure 3, $\sigma(X)$ versus X, the conductivity itself is decreasing at large X. This is possibly due to a change in the scattering mechanism.

The above analysis can also be applied to doping studies with a third element. In this case, X is replaced by A in equations (13) and (14). Figure 10 is a graph of $n(A)/n(68.03)$ versus A_{Cd} for cadmium
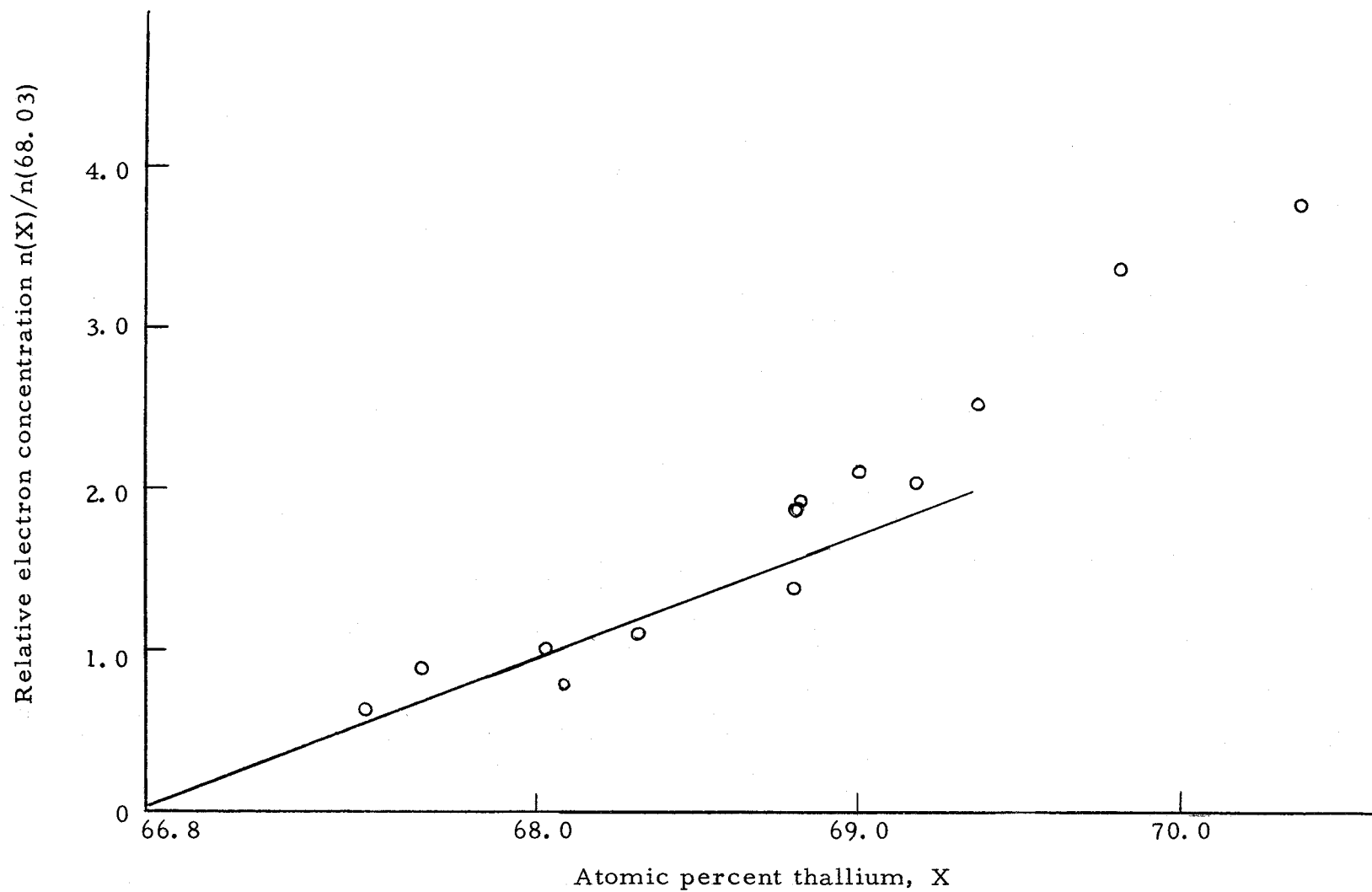
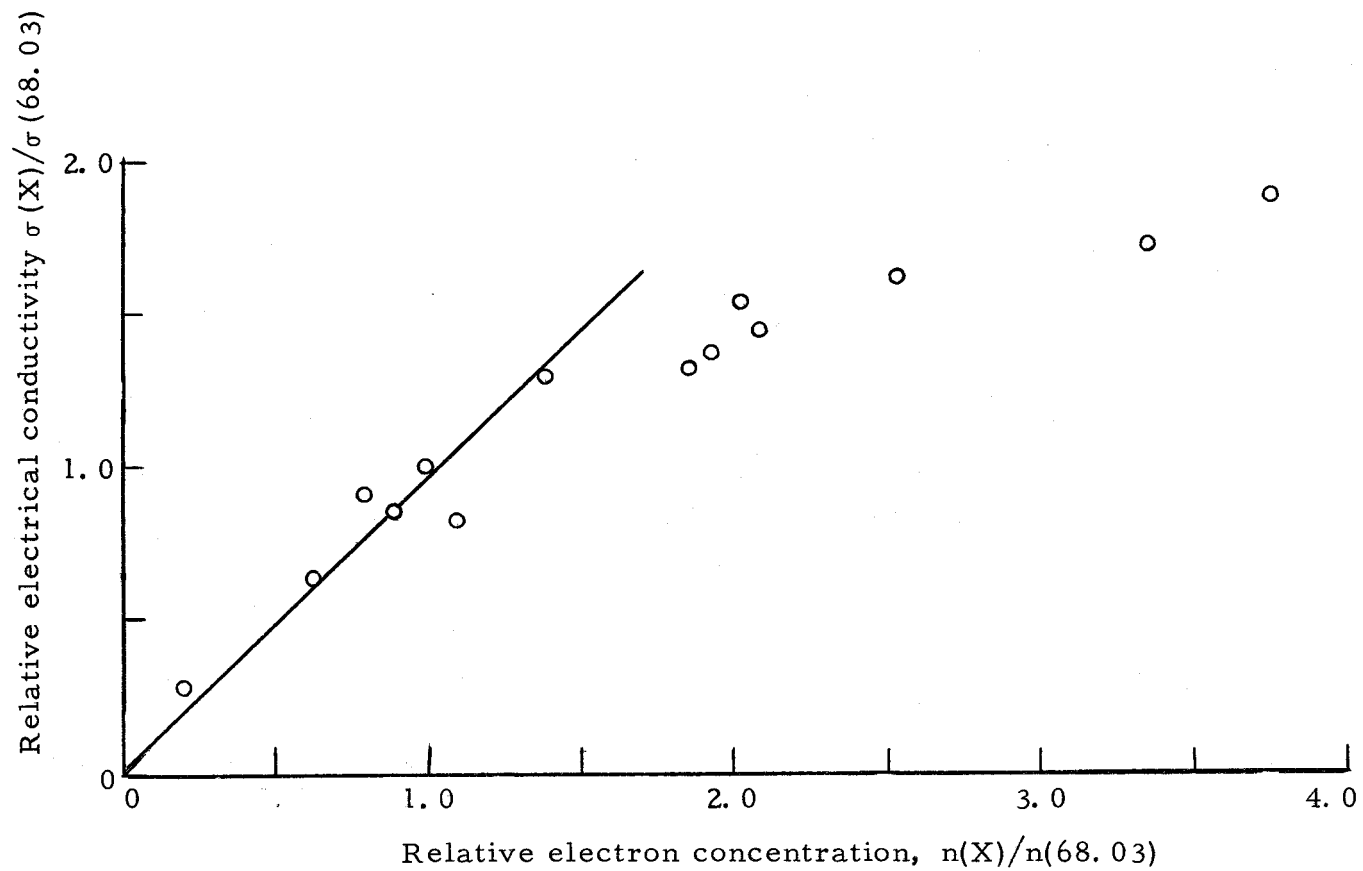Figure 8.   Relative electron concentration versus X.

Figure 9. Relative conductivity (at 800°K) versus relative electron concentration for thallium-tellurium solutions.
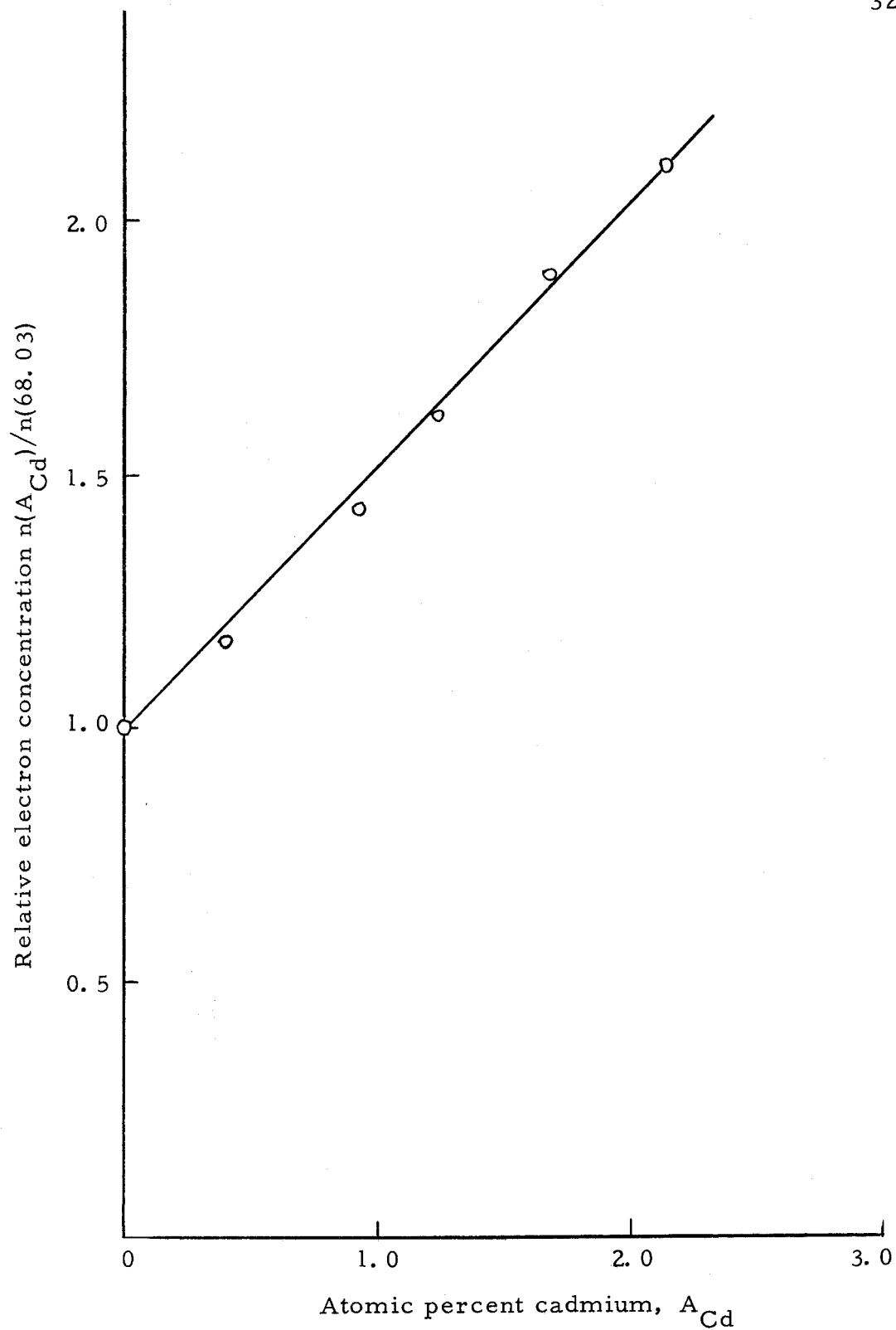
Figure 10. Relative increase in electron concentration for cadmium doped X68.03 solutions.

doping. The slight scatter around the straight line is consistent with the accuracy in measuring the Seebeck coefficient. Similar graphs for the other doping elements show straight lines, but with different slopes. The slope of these curves is used to calculate $(1/n(X_r))(dn(A_i)/dA_i)$, where X_r is a reference composition, which is a measure of the doping effectiveness of the elements. Table 2 lists the values of $(1/n(70.38))dn(A_i)/dA_i$ for the elements studied. Setting the "valence in solution" of thallium as unity, ratios of $dn(A_i)/dA_i$ to $dn(X)/dX$ provide an effective valence in solution for the five elements relative to thallium. Table 3 shows this ratio. The numbers in parentheses are the nearest integral fractions in which the decimals can be expressed. Indium, silver, and antimony are all one-quarter as effective as thallium as doping agents, although antimony removes electrons instead of adding them.

Table 2. Effect of doping elements on concentration.

Element	$[1/n(70.38)]dn(A_i)/dA_i$
Ag	0.078
Cd	0.110
In	0.086
Sn	0.174
Sb	-0.093
Tl	0.348

Table 3. Effective doping element valence.

Element	$[dn(A_i)dA_i]/[dn(X)/dX]$	
Ag	0. 225	(1/4)
Cd	0. 315	(1/3)
In	0. 246	(1/4)
Sn	0. 499	(1/2)
Sb	-0. 266	(-1/4)

Figure 11 shows $\sigma(A)/\sigma(68.03)$ versus A_{Cd} at T = 800° K for cadmium doping. The experimental points fall very well on a straight line. The other doping elements yielded equally good straight lines in similar graphs. As long as A_i was less than 2. 5 atomic percent the mobility showed no sign of being affected by the presence of the third element. Doping levels above about 2. 5 atomic percent caused the points to deviate from the straight line. Table 4 lists the values of $1/\sigma(70.38)(d\sigma(A_i)/dA_i)$ for the five doping elements and thallium. Thallium is the most effective in causing changes in the conductivity; silver is the least. One might be tempted to infer from the linear dependence of $\sigma(A)/\sigma(70.38)$ versus A that the mobility is independent of composition. This does not seem to be true, as indicated by the lack of correlation between the numbers in Table 2 and those of Table 4. This inconsistency suggests that the straight lines, such as in Figure 11, are not properly interpreted by equation 14.
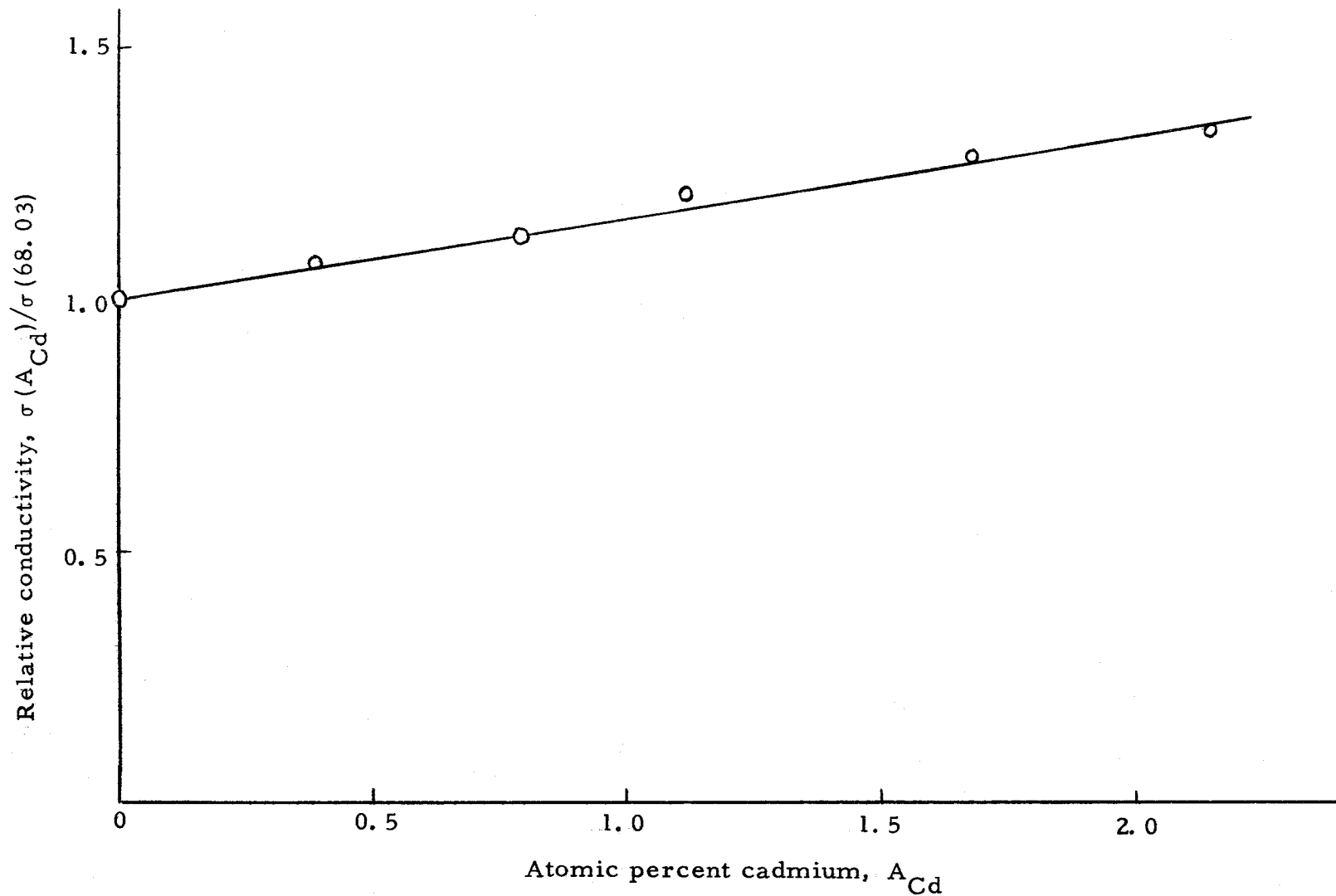
Figure 11. Relative increase in electrical conductivity for cadmium doped X68. 03 solutions at T = 800°K.

Apparently, μ also changes linearly with A. It is interesting to note that the elements in Table 4, when ranked in order of doping effectiveness, least effective to most effective, are in the same order as their atomic numbers.

Table 4. Effect of doping elements on electrical conductivity at 800°K.

Element	$[1/\sigma(70.38)][(d\sigma(A_i)/dA_i]$
Ag	0.067
Cd	0.077
In	0.118
Sn	0.123
Sb	-0.177
Tl	0.275

Near Intrinsic Region

Near the intrinsic composition (X66.7) the transport para-
meters reflect the increasing contributions of electron-hole pairs to
transport. In this region

$$\sigma = ne\mu_n + pe\mu_p,$$ (1)

but now,

$$n \sim p.$$ (19)

Maxwell-Boltzmann statistics are applicable under these conditions.
Equation (9) can then be written as

$$S = S_n + (S_p - S_n)\frac{\sigma_p}{\sigma}.$$ (20)

$S_p - S_n$ is a quantity which does not change with carrier concentra-
tion:

$$S_p - S_n = \frac{k}{e}(A_n + A_p + E_G/kT).$$ (21)

Holes are minority carriers in n-type thallium-tellurium solu-
tions; their presence is due to the thermal excitation of electrons
across the band gap. From an examination of the conductivity versus
temperature curves of n-type compositions in the near intrinsic
region we can draw some rough conclusions about the magnitude of
the energy gap. In a region in which the concentration of holes is
large enough to affect σ noticeably, but still much less than the con-
centration of ionized donor states, N,

$$n = N + p \sim N. \tag{22}$$

Write equation (2) as

$$p = \frac{C}{N} \exp(-E_2/kT). \tag{23}$$

C is a constant, and the temperature dependence of $N_c N_v$ is included in E_2. Equation (7) becomes

$$\sigma = \sigma_N + e\mu_n (1 + b)\frac{C}{N} \exp(-E_2/kT). \tag{24}$$

For these compositions $d\mu_n/dT$ is close to zero. Equation (24) then predicts that a graph of $\ln(\sigma - \sigma_N)$ versus T^{-1} should yield a straight line whose slope is $-E_2/k$. Figure 12 is such a graph of two compositions, X68.08 and X68.81, which were studied in a quartz cell. The activation energies, E_2, of these compositions are 0.45 and 0.72 electron volts, respectively. The latest paper by Cutler and Mallon (1966), from which the above analysis and notation were drawn, quotes a value of $E_2 = 0.65 \pm 0.10$ electron volts for the activation energy of two solutions for which they have high temperature data. These solutions were X68.2 and X68.4, as determined by fitting their conductivity data to the curve of $\sigma(X)$ versus X in Figure 3. The values of E_2 determined here are thus consistent with the previous results and show the decrease in magnitude for compositions close to the intrinsic region also noted earlier (Cutler and Mallon, 1966).
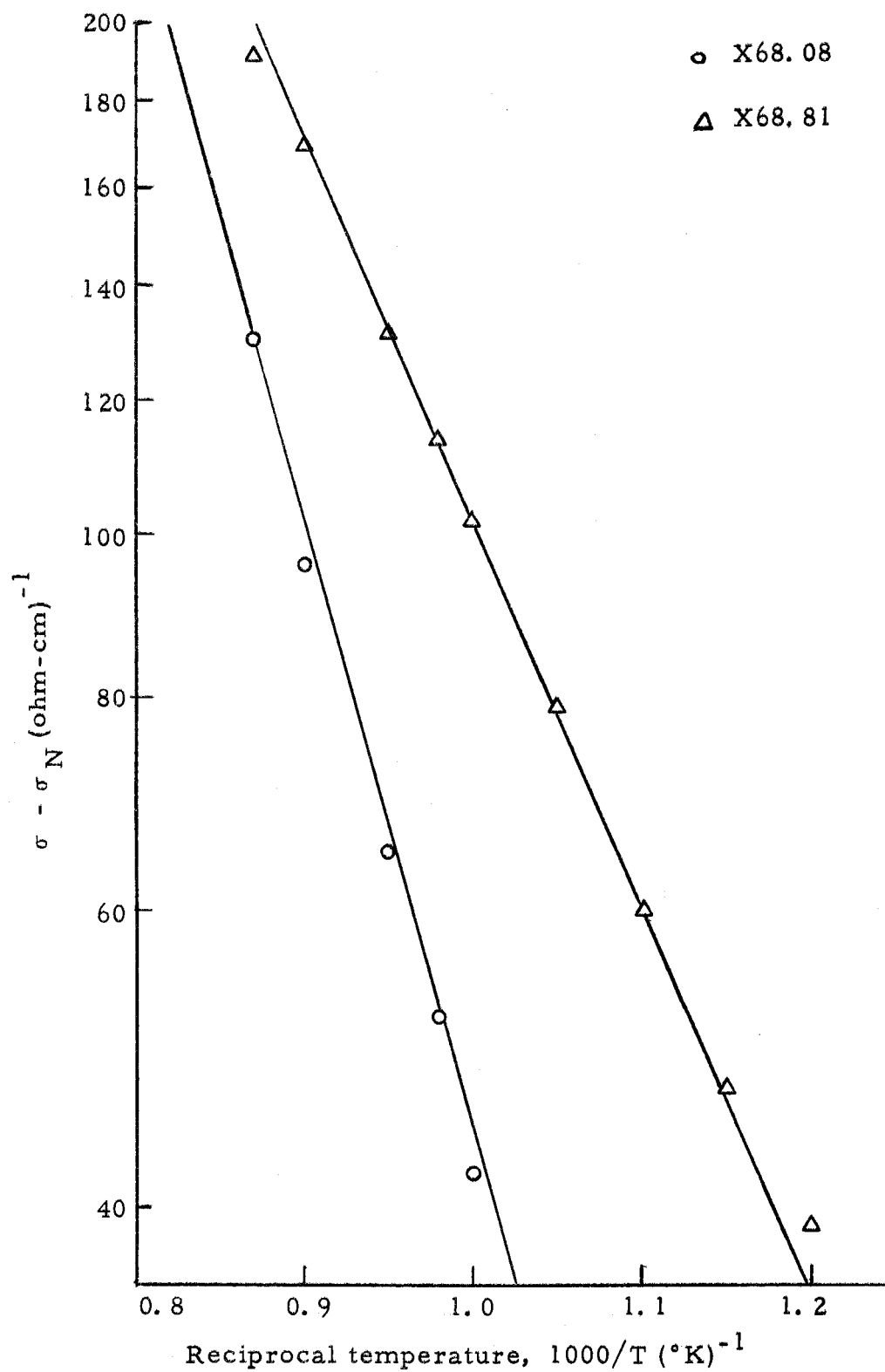
Figure 12.   Effect of thermal electron excitation in X68.08 and X68.81

During measurements on the p-type solutions X66. 5 and X66. 0 with quartz cells, p-n transitions were observed in the Seebeck coefficients of these melts at high temperature. At high temperatures

$$n \sim p \sim n_i. \tag{25}$$

In equation (10), then, $A_n = A_p$, since the scattering mechanism should be the same for holes and electrons. N_c and N_v differ only by the ratio of the effective mass of holes and electrons to the three-halves power. The logarithm of this ratio is probably a small number. Equation (9) can thus be written

$$S \cong \frac{S_i}{(\mu_n + \mu_p)} (\mu_p - \mu_n). \tag{26}$$

S_i is the common magnitude of S_n and S_p. Equation (26) shows that the thermoelectric power at high temperature will have the sign of the carrier whose mobility is largest. As the temperature is decreased and the approximation expressed in equation (25) becomes invalid, the sign of the Seebeck coefficient will again be dictated by the carrier whose concentration is largest. Figure 13 shows the p-n transition in X66. 0 and X66. 5 solutions at high temperature. The results in Figure 13 indicate that the electron mobility is larger than the hole mobility in liquid thallium-tellurium solutions. This is the usual result in solid semiconductors. Addition of small amounts of n-type impurities to X66. 0 caused a steady decrease in the temperature at which the p-n transition occurred. After adding 0. 40
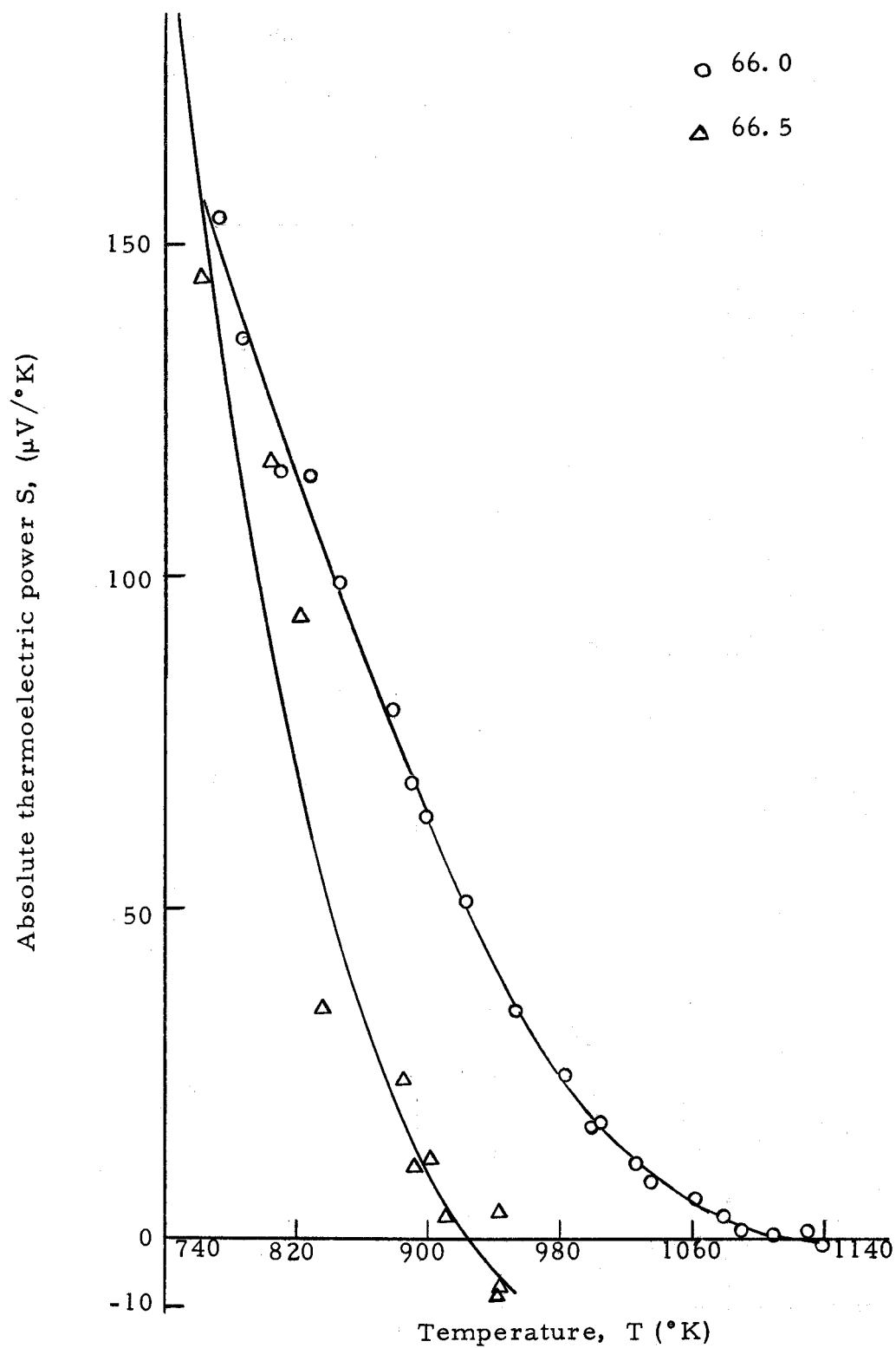
Figure 13. Seebeck coefficient p-n transitions at high temperature.

atomic percent indium to X66. 5, the Seebeck coefficient was driven

strongly n-type. This indicates again that the intrinsic composition

is only slightly larger than X66. 5.

The concentration of holes present in compositions above about

X68. 0 is very small at lower temperatures. This can be seen in

Figure 1, where the conductivity of these solutions is nearly inde-

pendent of temperature, Figure 3 shows that $\sigma(X)$, at $T = 800°K$,

is a linear function of X for a range X68. 0 to X69. 2, roughly. A

straight line through the data in this range, extrapolated to $\sigma = 0$

at $X_0 = 66. 7$, the intrinsic composition , might be expected to yield

the conductivity due to the ionized donor centers,

$$\sigma_N = e\mu_n N. \tag{27}$$

Also from Figure 3 we can obtain the intrinsic conductivity, σ_i,

which is the conductivity at $X = X_0$, the minimum conductivity:

$$\sigma_i = e(\mu_n + \mu_p)n_i. \tag{28}$$

The data then furnishes σ_i, X_0, σ_N, and $\sigma - \sigma_N$ as a function of X,

or N. Since

$$\sigma - \sigma_N = e(\mu_n + \mu_p)p, \tag{29}$$

it is possible to calculate from the experimental data the ratios of

the quantities in equations (27), (28), and (29) to yield the fractions

p/n_i, $\dfrac{p}{N} \dfrac{(b + 1)}{b}$, $\dfrac{b}{b + 1} \dfrac{N}{n_i}$, where $b = \dfrac{\mu_n}{\mu_p}$. These were compared with

the equilibrium relationship

$$(p + N)p/n_i^2 = 1. \tag{30}$$

It was found that the numbers obtained from the experimental data were inconsistent with equation (30). In fact, the analysis leads to negative values for the ratio μ_n/μ_p, which is impossible. A consideration of the probable chemical equilibrium between donor and acceptor centers near the intrinsic composition, X_0, indicates that the assumption of equation (13), that $N = a(X - X_0)$, is not likely to be correct in the vicinity of X_0. Therefore the deduction of σ_N from the straight line extrapolation in Figure 3 is incorrect. Near the intrinsic composition, N should be interpreted as the difference between the number of ionized donor centers and the number of acceptor centers:

$$N = N_D - N_A. \tag{31}$$

Because of chemical equilibrium between donor and acceptor states, the value of σ_N is expected to fall below the solid line shown in Figure 3 as X approaches X_0. This is consistent with the requirements of the experimental data in the light of equations (27) - (29).[1]

---

[1] Verbal communication from M. Cutler.

DISCUSSION AND CONCLUSIONS

We have presented the results of a detailed study of the electrical conductivity and Seebeck coefficient of extrinsic liquid thallium-tellurium solutions from X67. 0 to X72. 0, as summarized in Figures 1 and 2. These data extend the range of previous work (Cutler and Mallon, 1965), and reflect an improvement in the accuracy and reproducibility arising from new experimental techniques developed during the course of the investigation. The increased accuracy is particularly important on the n-type side, since the electrical properties are very sensitive to composition. It has been possible to fit the conductivities of some of the solutions studied by Cutler and Mallon (1965) to Figure 3 of this report, and thereby assign more accurate compositions to them. This has made the earlier data more useful.

As a result of the analysis presented, it appears that the electron mobility in n-type solutions is constant for compositions between X67. 0 and X68. 5. The mobility then apparently decreases at larger X. The decrease in μ_n at large X may be caused by impurity scattering, since the thallium atoms in excess of 66.7 atomic percent form ionized impurity states. Below X68. 5, then, the impurity states are apparently not dominating the scattering, since μ_n is constant. On the other hand, there is no evidence of a decrease in mobility with

increasing temperature, as would be expected for thermal scattering. The latter was observed on the p-type side by Cutler and Mallon (1966). If anything, μ increases with increasing temperature, approximately as T^a, where a is some number between 0.1 and 0.25. One possibility is that the dominant cause of scattering is the intrinsic disorder of the liquid "lattice".

The results of doping extrinsic n-type thallium-tellurium solutions with silver, cadmium, indium, tin, antimony, and bismuth show that the addition of these elements changed σ and S in a manner comparable to adding thallium or tellurium. All of the doping elements were less effective in changing σ and S than thallium on an atom for atom basis. The direction of the change in carrier concentration as a function of adding a third element was consistently one in which electropositive elements (Ag, Cd, In, Sn) lost electrons to the solution; electronegative elements (Sb, Bi) removed electrons. Therefore the pattern is one of creating impurity states by ionization. The nature of the impurity states is not clear; the relatively small efficiency in adding or removing electrons (compared to thallium) suggests possible coupling of several atoms to form one state. However, in no case was there a reversal such as is observed in germanium and silicon, where some elements more electropositive than the host atom form acceptor states and vice versa (Fan, 1955). The overall behavior of S and σ as a function of doping agent is qualitatively

consistent with conventional theory. The electrical conductivity increases and $|S|$ decreases when the electron concentration is increased. The deduction for the quantitative behavior of the electron concentration, n, from the behavior of S is based on the assumption that the scattering parameter r is not changing appreciably. Since the mobility is apparently changing when a third element is added, there may be some question about this assumption. However, it seems likely that for small amounts of the third element, the overall change in r will be small compared to the chance in n (and hence S). Most of the scattering in the doped liquid is caused by the same mechanism as in the original liquid. Therefore, one may expect the change in n on adding impurities to have a first order effect on S, and the change in scattering to have a second order effect.

In addition to the above, other observations and results were reported which augment other information and help add to an understanding of these liquid semiconductors. Among these, (1) the liquidus of the phase diagram was explored to some degree between X60 and X72, (2) some activation energies were calculated for n-type, near intrinsic compositions, and (3) p-n transitions in the Seebeck coefficient at high temperatures have indicated that $\mu_n > \mu_p$.

With the development of reliable quartz cells capable of extending this work to temperatures near 1000°C, there are several experiments of interest which could be performed. Data on the conductivity

and Seebeck coefficient for a sufficiently wide temperature interval could be matched to theoretical curves for the temperature dependence of σ and S. This might yield better information about the scattering mechanisms. In the intrinsic region, a careful study of the temperatures where the p-n transitions occur may also shed some light on the scattering mechanisms.

Further work which could be done with the present apparatus would be an investigation of other elements in the periodic table in doping thallium-tellurium solutions. It would be interesting, and perhaps informative, to find out whether copper, zinc, gallium, and germanium acted similarly to silver, cadmium, indium, and tin, respectively. In the same vein, arsenic could be compared with both antimony and bismuth.

BIBLIOGRAPHY

Blakemore, John Sydney. 1962. Semiconductor statistics. New York, Pergamon Press. 381 p.

Cutler, M. and J.F. Leavy. 1963. Liquid semiconductors: an exploratory study. San Diego. 38 numb. leaves. (General Atomic Corporation. General Atomic Report GA-4420)

Cutler, M. and C.E. Mallon. 1965. Thermoelectric properties of liquid semiconductor solutions of thallium and tellurium. Journal of Applied Physics 36:201-205.

Cutler, M. and C.E. Mallon. 1966. Electronic properties of liquid semiconductor solutions of thallium and tellurium. The Physical Review 144:642-649.

Elliot, Rodney P. 1965. Constitution of binary alloys, first supplement. New York, McGraw-Hill. 877 p.

Fan, H. Y. 1955. Valence semiconductors, germanium and silicon. In: Solid state physics, ed. by Frederick Seitz and David Turnbull. Vol. 1. New York, Academic Press. p. 284-365.

Ioffe, A. F. and A. R. Regel. 1960. Non-crystalline, amorphous, and liquid electronic semiconductors. In: Progress in semiconductors, ed. by Allan F. Gibson. Vol. 4. New York, Wiley. p. 239-291.

Kittel, Charles. 1960. Introduction to solid state physics. 2d ed. New York, Wiley. 617 p.

Seitz, Frederick. 1940. The modern theory of solids. London, McGraw-Hill. 698 p.

Stoneburner, D. F. 1965. Thermoelectric power and electrical conductivity of molten binary thallium alloys. Transactions of the Metallurgical Society of AIME 233 (1): 153-159.

APPENDICES

APPENDIX 1.   EXPERIMENTAL TECHNIQUES

Cutler and Mallon (1965) have discussed thoroughly the design criteria and construction details of the Seebeck cell.   Our cell design differed in no important respect from theirs.   Some small improvements were made which increased the ease of operation or accuracy of the results.   We found it desirable to minimize the length of the electrode region (A, Figure 14), because near 600°C the viscosity of pyrex decreases appreciably.   As the glass softened, the torque exerted by a long electrode region deformed the cell.   The length of the tungsten electrodes and their depth of penetration into the cell were made as small as possible. This was done to counteract the effect of any temperature gradient along the length of the tungsten lead through which would cause an inaccuracy in the temperature reading.   The thermocouples themselves were of small diameter (0.010") so as to minimize the conduction of heat away from the junction.   The thermocouples were checked between zero degrees celsius and one hundred degrees celsius before and after each experiment. Any pair of thermocouples whose reading deviated more than one-half degree between those temperatures was discarded.

In this experiment it was necessary to exclude as much oxygen as possible from the cell.   The argon gas used in backfilling the cell was purified by flowing through a sealed cartridge containing hot titanium

ribbon. The hot ribbon removed most of the oxygen from the gas as determined by actual test. The thallium, after flowing through glass funnels to remove oxide, is stored in a small glass test tube for later casting into the cell.

A procedure was invented for cleaning glassware which seemed to be effective in reducing cell breakage. Before each measurement the cell was washed with a strong KOH solution, etched with three percent HF - two percent HNO_3 - 95 percent HOH, rinsed well with distilled water and alcohol, and then baked at 300°C under a vacuum for several minutes. This routine seemed to inhibit bonding between the glass and the frozen alloy, possibly by changing the glass surface in some undetermined fashion.

An accurate knowledge of the composition of the solutions studied can be obtained by depositing accurately known amounts of the elements into the cell. Tellurium does not oxidize readily at room temperature, and could be simply weighed and poured into the cell at the beginning of a measurement. Thallium was introduced into the cell by the following method: a glass test tube of known empty weight was filled with clean thallium under a vacuum. The test tube was then inverted in a long pyrex cylinder open at both ends, but tapered at one end so that the test tube could not fall through. The pyrex cylinder was inserted into the cell, the system was heated while flowing dry argon past the cell mouth and over the thallium.

When liquid, the thallium ran into the cell reservoir without touching

the tapered pyrex cylinder. The test tube could be withdrawn and re-

weighed after use. In this manner, known amounts of clean thallium

could be inserted into the cell.

Precise amounts of a third element or tellurium were added to

the melt in much the same way as above. Referring to Figure 14,

the end stop on the cell cap, B in the figure, was removed while

flowing argon gas through the stopcocks shown. The flow (C to D to

E) was used as a buffer: vapor from the hot melt stayed in, and air

stayed out. A detachable crucible on a long stainless steel handle

(F) would be inserted at B. As the furnace was rotated the material

in the crucible would slide into the liquid. Weighing the crucible

before and after use allowed a satisfactory control over the composi-

tion.

Quartz Seebeck cells were constructed to the same design as

those of pyrex. The tungsten electrodes were sealed through the

quartz with a sealing glass manufactured by the General Electric

Company. The technique required to obtain a satisfactory seal is

difficult, and demands a skillful glassblower. There were two major

difficulties with the quartz cells of this design. In order to seal the

tungsten into the cell a large amount of the sealing glass had to be

molded around the tungsten. This led to an excessive distance be-

tween the points at which the electrode was in contact with the liquid

CELL

Not to scale

Electrodes

Reservoir

X

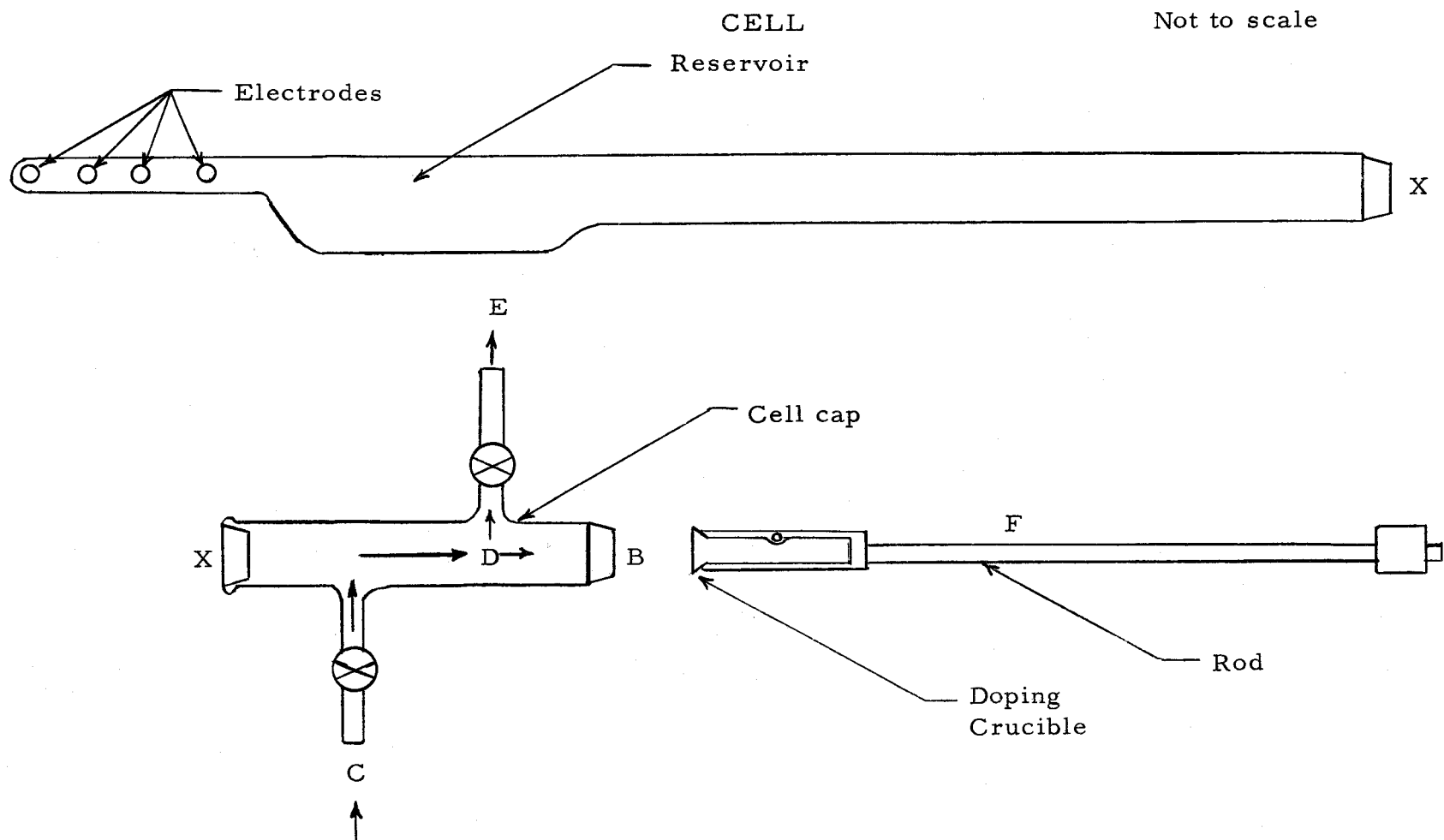E

Cell cap

X

D

B

C

F

Rod

Doping
Crucible

Figure 14.   Seebeck cell and doping apparatus.

and with the thermocouples. As a result, the thermocouples were not indicating the true temperature of the liquid. Consequently, the thermoelectric measurements in quartz cells did not agree with data from pyrex cells for the same compositions. This difficulty might be overcome with a more careful design. The second problem was noticed after a quartz cell had been heated several times to temperatures approaching 900°C. After several cycles the quartz cells would yield erratic, non-reproducible values of both the Seebeck coefficient and the resistivity. This was attributed to corrosion of the tungsten electrodes by the melt at high temperatures. This is a serious problem, and one which will probably only be solved by using carbon or graphite electrodes.

APPENDIX 2.   DERIVATION OF THE
SEEBECK COEFFICIENT

We will derive here the expression for the Seebeck coefficient using conventional transport theory.   An effort will be made to point out some of the assumptions built into the equations.

A solution of the Boltzmann equation assuming a relaxation time, τ, gives, for nondegenerate semiconductors, (Fan, 1955),

$$S = \frac{k}{q}(\log \frac{N_a}{n} + K_2/K_1).$$

A(1)

N_a is the effective density of states.   From this point on the discussion will refer to electrons, in which case,

$$N_a = N_c = 2(2\pi m_n^* kT)^{3/2}/h^3,$$

A(2)

$$K_n = \frac{1}{4\pi^3} \int v_x^2 E^{n-1} \tau (\partial f_0 / \partial E) d\Omega_k.$$

A(3)

f_0 is the unperturbed Fermi-Dirac distribution function,

$$f_0 = \frac{1}{1 + \exp[(E - E_f)/kT]}$$

A(4)

The following assumptions are made immediately:

$$\tau = \tau_0 E^r,$$

$$v_x^2 = \frac{2}{m} \frac{E}{3}.$$

Then,

$$K_n = \frac{2\tau_0}{12m\pi^3} \int E^{n+r} \frac{\partial f_0}{\partial E} 4\pi k^2 dk.$$

But

$$4\pi k^2 = 2\pi \frac{(2m)^{3/2}}{\hbar^2} E^{1/2} dE. \qquad A(5)$$

Thus

$$K_n = \frac{2}{3} \frac{\tau_0}{m} \frac{(2m)^{3/2}}{\hbar^2} \frac{1}{4\pi^2} \int E^{n+r+\frac{1}{2}} \frac{\partial f_0}{\partial E} dE.$$

Integrating the parts,

$$K_n = (r + n + 1/2)\tau_0 \frac{(2m)^{3/2}}{\hbar^2} \int E^{r+n-1/2} f_0 \, dE. \qquad A(6)$$

Let us define the dimensionless variables

$$x \equiv E/kT,$$

$$\zeta \equiv E_f/kT.$$

This leads to

$$K_n = (r + n + 1/2)\tau_0 \frac{(2m)^{3/2}}{\hbar^2} (kT)^{r+n+1/2} \int_0^\infty \frac{x^{r+n-1/2} dx}{1 + \exp(x-\zeta)}. \qquad A(7)$$

The integral corresponds to tabulated functions, the Fermi-Dirac

integral (Blakemore, 1962)

$$F_j(\zeta) = \frac{1}{\Gamma(j+1)} \int_0^\infty \frac{E^j \, dE}{1 + \exp(E - \zeta)}. \qquad A(8)$$

The expression $\Gamma(j+1)$ is a gamma function. Using A(7) and A(8),

$$K_2/K_1 = (r + 5/2)kT \frac{F_{r+3/2}(\zeta)}{F_{r+1/2}(\zeta)}.$$

Therefore,

$$S_n = - \frac{k}{e} \left[(r + 5/2) \frac{F_{r + 3/2}(\zeta)}{F_{r + 1/2}(\zeta)} - \zeta \right] . \qquad A(10)$$

The Fermi-Dirac integrals have been tabulated by Blakemore (1962) and others.

An analytical expression for the concentration of occupied electron states is derived below.

$$n = \frac{1}{4 \pi^3} \int \frac{d\Omega_k}{1 + \exp[(E - E_f)/kT]} . \qquad A(11)$$

As before,

$$d\Omega_k = 4 \pi k^2 dk,$$

$$E = \frac{\hbar^2 k^2}{2m} ,$$

$$4 \pi k^2 dk = 2 \pi \frac{(2m)^{3/2}}{\hbar^2} E^{1/2} dE.$$

Then

$$n = \frac{1}{2 \pi^2} \frac{(2m)^{3/2}}{\hbar^2} \int_0^\infty \frac{E^{1/2} dE}{1 + \exp[(E - E_f)/kT]}$$

Let

$$x \equiv E/kT,$$

$$\zeta \equiv E_f/kT.$$

$$n = \frac{(2mkT)^{3/2}}{\hbar^2} \frac{1}{2 \pi^2} (kT)^{3/2} \int_0^\infty \frac{x^{1/2} dx}{1 + \exp(x - \zeta)} . \qquad A(12)$$

Now,

$$N_c = 2(2\pi m_n^* kT)^{3/2}/h^3. \qquad\qquad A(2)$$

Therefore

$$n = N_c F_{1/2}(\zeta), \qquad\qquad A(13)$$

using equations A(8) and A(12).

In applying these results, equations A(10) and A(13), arbitrary values are chosen for n, say $n = 1.484 \times 10^{20}$ cm^{-3}, m^* (=m), and a value of r. Using these, a theoretical curve of S versus ln T is plotted which corresponds to equation (11). In the Maxwell-Boltzmann limit where $-\zeta \gg 1$, equation A(10) reduces to

$$S_n = -\frac{k}{e}\left[A_n + \ln(N_c/n)\right], \qquad\qquad A(14)$$

with $A_n = r + 5/2$. From equation A(14) it is obvious that changing the value of m^* or r would only shift the theoretical curve horizontally. This remains true for the analogous equations A(10) and A(13) for a different m^*, and nearly so for r, in the almost degenerate extrinsic region where most of the data lies. (See Blakemore, 1962, Appendix C.)